

Internal conversion and the evolution of nuclear structure at very high spin: ^{154–158}Er

T. M. Cormier, P. M. Stwertka, M. Herman, and N. G. Nicolis

*Department of Physics and Astronomy and Nuclear Structure Research Laboratory,
University of Rochester, Rochester, New York 14627*

(Received 17 April 1984)

The atomic charge state distributions of ^{154–158}Er ions produced in fusion reactions with ³²S and ³⁴S beams and ^{126–130}Te targets are used to deduce the average internal conversion probabilities of continuum γ transitions at high spin. A strong dependence is observed on both neutron number and spin. For each of the nuclei ^{155–158}Er a critical spin is observed at which a sudden enhancement of internal conversion occurs. This result alone implies either a sudden enhancement of $M1$ radiation, a sudden decrease of the average $E2$ transition energy, or some mixture of the two. In either case a major change in the underlying structure of the rotating body is implied. Previous continuum γ -ray spectroscopy measurements support the interpretation involving enhanced $M1$ radiation at very high spin.

I. INTRODUCTION

Experimental techniques aimed at probing the structure of nuclei at very high spin have improved and expanded dramatically in recent years. The study of resolved transitions up to $J \lesssim 40\hbar$ is now possible in many cases. Beyond this spin and up to spins at which the fission barrier vanishes it is still necessary, however, to study the properties of nuclei averaged over several bands. Indeed, virtually all of our present understanding of the properties of nuclei at the very highest spins has come from such studies.¹ By its nature such so-called continuum spectroscopy studies are less precise than conventional spectroscopy. For this reason it is frequently essential to view the same phenomenon from several independent perspectives in order to gain several different insights into a problem. In the present work, the energy dependence of the atomic charge state distributions of fusion evaporation residues are used to infer the spin dependence of average continuum internal conversion probabilities. These probabilities are a sensitive indicator of the evolution of nuclear structure with spin.

Recently, there has been renewed interest in the structure of nuclei with $64 \leq Z \leq 72$ and $82 \leq N \leq 90$. The interest in this region was first spurred by the discovery of an island of high spin yrast isomers and the complementary observation of a double shell closure at ¹⁴⁶Gd₆₄. The renewed interest, however, derives largely from an extensive theoretical survey of nuclear structure in this mass region at very high spin. Cranked shell model calculations, for example,² predict equilibrium nuclear shapes which evolve dramatically as a function of spin through prolate, oblate, and triaxial shapes. The exact sequence of shapes predicted, the spins at which shape transitions occur, and the equilibrium deformations are strongly dependent on neutron number but are less sensitive to proton number. A consistent feature of these calculations is the prediction of a prolate to oblate shape transition at spins ranging from $J \simeq 20\hbar$ at $N = 86$ to $J \simeq 50\hbar$ at $N = 90$. There is un-

doubtedly a considerable model dependence in the calculated values of the transition spins but the qualitative result that the transition spin increases with neutron number is well established within the theory.

The observable consequences of a prolate to oblate shape transition at high spin have been discussed by Peker *et al.*³ The deexcitation of a prolate rotor proceeds mainly via stretched electric quadrupole ($\Delta J = 2$) transitions. From a state of spin J , these transitions have an energy

$$E_\gamma = \frac{\hbar^2}{2I_p}(4J - 2), \quad (1)$$

where I_p is the effective moment of inertia in the prolate shape. Spin-energy correlated transitions consistent with Eq. (1) have been observed¹ in a variety of heavy ion reactions leading to the rare earth region and γ -ray angular distributions have been used to suggest the dominance of quadrupole radiation. The alignment of the compound nucleus in (HI,xn) reactions is largely retained through the neutron emission process and subsequent γ decay resulting in an anisotropy of $W(0^\circ)/W(90^\circ) \simeq 1.4 - 1.5$ for the quadrupole radiation.

γ decay in a region of oblate equilibrium shapes is more complicated. For small oblate deformations, single particle transitions dominate. At very high spin, however, where the oblate shape is the result of the alignment of many quasiparticle orbits, a larger deformation is likely and collective transitions are again possible. One class of states involved results from rotations of the oblate body perpendicular to its symmetry axis or wobble of the symmetry axis and spins $J = K, K + 1, K + 2, \dots$, are obtained. Clearly, in this picture, K is a large number and this in turn determines the dominant multipolarity of the γ cascade. The large K limit of the rotational model matrix elements gives $B(M1) \sim K^2$ while $B(E2) \sim 1/K$. Thus, at sufficiently high spin the deexcitation of the oblate rotor will proceed with a significant $M1$ component. Indeed, close to a band head ($J \simeq K$), $M1$ radiation is ex-

pected to dominate.

Identification of an $M1$ component in the continuum γ spectrum has previously been based on its energy and anisotropy. The energy of the $M1$ transition from a state of spin J is

$$E_{\gamma} = \frac{\hbar^2}{2I_0}(2J), \quad (2)$$

where I_0 is the effective moment of inertia in the oblate shape. In the very high spin region of interest here, the effective moments of inertia are already very close to the rigid body value. Thus, we expect that $I_0 \simeq I_p$ for collective transitions and hence the average γ -ray transition energy in an oblate region will be approximately $\frac{1}{2}$ the corresponding transition energy in the neighboring prolate region.

Anisotropies in the range of 0.5–1.0 are conventionally associated with dipole transitions. At the highest energies in the continuum γ spectrum these are predominantly $E1$ (statistical) transitions while at energies below those characteristic of the $E2$ transitions, evidence for $M1$ radiation has been observed.⁴

In a few selected cases up to moderate spins, the assignment of multiplicities in the continuum based on γ -ray anisotropies has been checked by direct measurement of the continuum internal conversion electron spectrum.⁵ These measurements yield average internal conversion coefficients as a function of γ -ray transition energy.

The most recent measurements of γ -ray continuum spectra using the Oak Ridge spin spectrometer⁶ have begun to address the questions of nuclear shape evolution at high spin. In particular, Jaaskelainen *et al.*⁷ have recently reported a study of $^{157-161}\text{Yb}$ in the range of $J = 15 - 55 \hbar$. Their measurements consist of γ -ray transition spectra measured with an array of 72 NaI detectors. For each of the isotopes ^{157}Yb – ^{161}Yb , γ spectra as a function of γ -ray multiplicity and angle have been measured. Using standard statistical model calculations, γ -ray multiplicity can be related to the spin J of the entry region.

As a function of J the γ -ray spectra of the Yb isotopes evolve as expected for rotors of medium deformation. Both the angular anisotropies and the variation of E_{γ} with J are consistent with dominant $E2$ radiation. For each isotope, however, a specific spin is observed at which the γ -decay characteristics change abruptly. Above this critical spin, strong dipole competition is observed with the strength of the dipole component being greater in the lightest isotopes. It is suggested⁷ that the dipole component signals the expected $M1$ radiation following the predicted prolate to oblate transition. Indeed the critical spins at which the dipole radiation first appears vary with isotope in qualitative accord with theory ranging from $J = 36\hbar$ at ^{157}Yb to $J = 50\hbar$ at ^{161}Yb .

Two features of the data of Jaaskelainen *et al.* are particularly striking. First, the dipole transitions are localized at $\frac{1}{2}$ of the energy of the corresponding $E2$ transitions, indicating continued collective rotation. With the exception of ^{158}Yb the dipole radiation is observed to persist through the highest spins reached in their experiment. In ^{158}Yb , however, the dipole component appears at $J \simeq 38\hbar$ and accounts for 50% of all transitions between

$J = 38\hbar$ and $48\hbar$. Above spin 48, the dipole component abruptly disappears and the decays at higher spin again proceed with stretched $E2$ radiation. The interval over which the dipole radiation is visible is remarkably narrow, especially in view of the finite angular momentum resolution of the spin spectrometer.

Jaaskelainen *et al.* interpret their ^{158}Yb data in terms of a transition to an oblate shape at $J \simeq 38\hbar$ with deformation $\epsilon = 0.25 - 0.3$ followed by a rapid transition to a strongly deformed triaxial shape beginning at $J = 48\hbar$. They suggest that the deformation reaches values as large as $\epsilon = 0.5$ by $J = 52\hbar$. This sequence of shapes is again in qualitative accord with theory. There are, however, serious quantitative discrepancies between theory and experiment. Within the cranked shell model the oblate shape, which is reached at $J = 30\hbar$, has a deformation $\epsilon < 0.1$, while the superdeformed triaxial configuration does not appear until $J > 70\hbar$. It is not clear at this time whether the existing theoretical framework will eventually account for these data or whether some new phenomenon is waiting to be identified.

Motivated by the experiments of Jaaskelainen *et al.*, the present paper reports on a study of the very high spin properties of $^{154-158}\text{Er}$. By studying the atomic charge state distributions of the fusion evaporation residues we deduce the internal conversion probabilities (α) of continuum γ transitions as a function of spin. Unlike conventional internal conversion measurements which determine α as a function of γ -ray transition energy, the present method is more directly applicable to the identification of new decay modes which appear and disappear as a function of spin. Internal conversion probabilities alone do not determine the multipolarity, of course. In addition, the γ -ray transition energy must be known. We have, therefore, measured the spin dependence of the continuum γ -spectrum in the case of ^{156}Er . On the whole, our data are consistent with the observation of strong $M1$ radiation at very high spin. Indeed, we find that the evolution of our internal conversion probabilities with J closely parallels the evolution of the γ spectra in the appropriate isotope of the Yb nuclei studied by Jaaskelainen *et al.*

II. EXPERIMENTAL METHOD

Fusion reactions of $^{32,34}\text{S}$ projectiles with $^{126,128,130}\text{Te}$ targets were used to produce $^{154-158}\text{Er}$ products via $3-7n$ reactions. Beam energies in the range of 115–170 MeV were used with intensities in the range of 10 particle nA to 0.05 particle nA. The targets were enriched to $>97\%$ in all cases and were $\simeq 150 \mu\text{g}/\text{cm}^2$ thick with $10 \mu\text{g}/\text{cm}^2$ ^{12}C backings. The targets were oriented with the ^{12}C backing downstream such that the recoiling erbium exits into vacuum after passing through the ^{12}C layer.

The heavy reaction products were detected at zero degrees with a recoil mass spectrometer^{8,9} which separated products according to mass and atomic charge state along a position sensitive gas detector at the focal plane. Figure 1 shows a schematic layout of the spectrometer. The instrument consists of two magnetic quadrupole triplet lenses (Q_1 – Q_6), two high voltage electrostatic deflectors ($E1$, $E2$), and one dipole magnet ($D1$). The distance

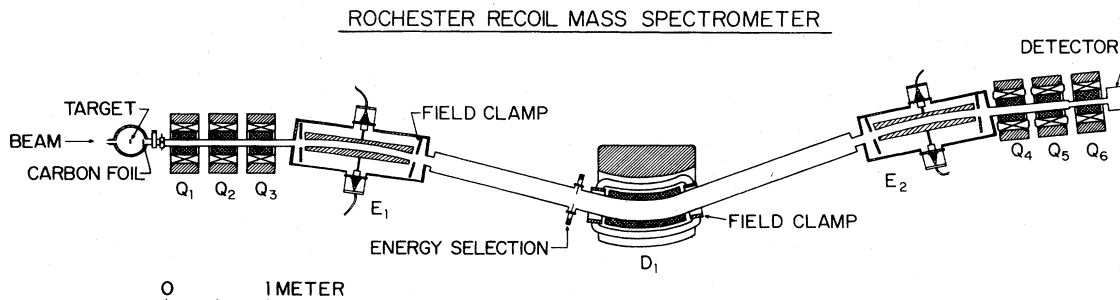


FIG. 1. Layout of the recoil mass spectrometer.

from the target to the detector is ≈ 11 m. The electric and magnetic fields are arranged in a velocity dispersion matching configuration as in a conventional Aston spectrometer.¹⁰ In the present device, however, approximate second order velocity focusing is achieved with an appropriately shaped magnetic field. As a consequence, $> 75\%$ of the entire evaporation residue energy spectrum can be transported to the focal plane for one atomic charge state at a time. Using several settings of the spectrometer fields, the entire atomic charge state distribution for each of the reaction product masses can be measured.

Figure 2 shows a typical mass spectrum measured for the $^{32}\text{S} + ^{130}\text{Te}$ reaction at 130 MeV. This spectrum was measured at atomic charge state $Q = 15^+$. The mass resolving power illustrated in this figure is $M/\Delta M \approx 425$. This resolution is largely due to the residual second order velocity dispersion of the spectrometer. By measuring the energy of the evaporation residues in the focal plane detector, an off-line correction for the residual velocity dispersion can be made which results in resolving powers in the range of 750. This correction procedure was not required in the present experiment, however.

Reaction products recoil into vacuum after a time of $\approx 7 \times 10^{-15}$ s. This time is much greater than typical

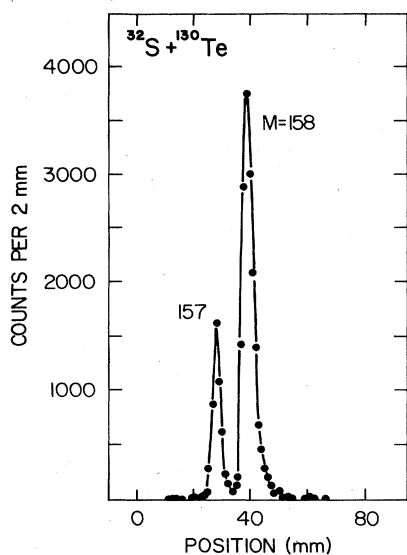


FIG. 2. A sample mass spectrum for the $^{32}\text{S} + ^{130}\text{Te}$ reaction at $E_{\text{lab}} = 130$ MeV. For this measurement the spectrometer was set for atomic charge state 15^+ .

atomic lifetimes in the inner shells but much shorter than typical nuclear γ -decay lifetimes. Reaction products therefore exit the carbon backing of the target into vacuum with an approximately equilibrated atomic charge state distribution. The nuclear γ decay, however, proceeds in vacuum, and barring the existence of long-lived isomers, is finished by the time the reaction product has recoiled a distance of a few mm from the target.

During the γ -decay cascade the atomic charge state distribution of an ion will be modified by any internal conversions which occur within the cascade. The effect of a single internal conversion on an ion isolated in vacuum is quite significant. In addition to the inner shell vacancy created by the internal conversion itself, the relaxation of the vacancy is normally accompanied by 4–5 Auger transitions. Thus, a single internal conversion raises the mean atomic charge state of an ion by 5–6 units. Furthermore, since the atomic inner shell vacancy is filled in a time much shorter than nuclear γ -decay times, the effect will be approximately additive for multiple internal conversions until the ion becomes so highly charged that the outer electrons are too tightly bound for multiple Auger decay to take place. It is thus possible, in principle, to determine the total number of internal conversions in a γ -decay cascade from the observed shift in the mean atomic charge state of the reaction products provided the number of converted γ transitions is not too large. Such a method is equivalent to the measurement of the multiplicity of characteristic (K, L, M) atomic x rays.¹¹ On the other hand, this method is also not suitable if there is, on the average, significantly less than one internal conversion in the decay cascade. The reason is that the shifted component of the charge state distribution is difficult to separate from the nonshifted component with sufficient precision to study variation of the internal conversion probability with spin. The erbium isotopes studied in the present work fall into this latter category. That is, being reasonably good rotors, the net internal conversion probability integrated over the entire γ cascade which may contain as many as 30 transitions is on the order of $\frac{1}{2}$. The largest single contribution to this probability comes from the lowest lying transition in the cascade and, therefore, the contribution to this probability coming from the transitions of interest at the top of the cascade is very small. In order to deduce the total internal conversion probability with sufficient precision to identify changes due to transitions at the highest spin we have developed the following method. A second carbon foil is mounted on a

precision remote positioning mechanism, a distance of 15 cm after the target. The second foil, which is removed and inserted under computer control, is encountered by reaction products after a time delay of ≈ 25 ns. At this point, the nuclear γ decay and associated internal conversions are finished and the second foil reestablishes the equilibrium atomic charge state distribution. Sample atomic charge state distributions for ^{158}Er ions produced in $^{32}\text{S} + ^{130}\text{Te}$ reactions at 130 MeV are shown in Fig. 3(a). Measurements made with $[\sigma_{\text{in}}(Q)]$ and without $[\sigma_{\text{out}}(Q)]$ the second carbon foil are shown. The influence of the converted γ decays is evident in the excess of high charge states visible in $\sigma_{\text{out}}(Q)$. The measured $\sigma_{\text{in}}(Q)$ curve is associated with the equilibrium atomic charge state distribution

$$\sigma_{\text{in}}(Q) = \sigma_{\text{eq}}(Q), \quad (3)$$

while for $\sigma_{\text{out}}(Q)$ we write

$$\sigma_{\text{out}}(Q) = (1-P)\sigma_{\text{in}}(Q) + P\sigma_{\text{ne}}(Q). \quad (4)$$

In Eq. (4) P is the probability that at least one internal conversion has occurred in the γ cascade and $\sigma_{\text{ne}}(Q)$ is the nonequilibrium charge state distribution which results following ≥ 1 internal conversions.

The functional dependence of $\sigma_{\text{ne}}(Q)$ is, in principle, quite complicated. Fortunately, in order to deduce P we need only take advantage of the fact that $\sigma_{\text{ne}}(Q)$ is shifted at least 5–6 units of charge higher than $\sigma_{\text{eq}}(Q)$. As a consequence, the ratio

$$\frac{\sigma_{\text{out}}(Q)}{\sigma_{\text{in}}(Q)} = (1-P) + P \frac{\sigma_{\text{ne}}(Q)}{\sigma_{\text{eq}}(Q)} \quad (5)$$

tends toward the constant value $1-P$ at low Q . This is illustrated in Fig. 3(b) for the experimental data for ^{158}Er of Fig. 3(a). It is thus possible to extract the total internal conversion probability for the entire γ cascade directly from the experimental data.

Indeed, P can be measured quite precisely if precautions are taken to control random errors. The main source of such errors is usual sensitivity of zero degree measurements to the detailed beam geometry. To control these errors, targets were evaporated in 1 mm diam spots onto the carbon backing while the direction of the beam at the target was continuously monitored with an array of four Si detectors mounted symmetrically around the beam at an angle of 20 deg. Residual fluctuations related to the beam or the spectrometer can be easily averaged over by cycling the second carbon foil in and out under computer control with a 40 s period. An automatic beam interrupt and data collection inhibit is used while the second foil is being moved. The reproducibility of the position of the second foil was found to be ≈ 0.01 mm.

With these precautions we find that measurements of P were reproducible within counting statistics. Except at energies where the cross sections become very small, counting statistics were typically 0.5%.

Two sources of systematic errors were considered. First, when the second carbon foil is placed in the path of the reaction products the detection efficiency of the spectrometer is reduced slightly as a result of multiple scatter-

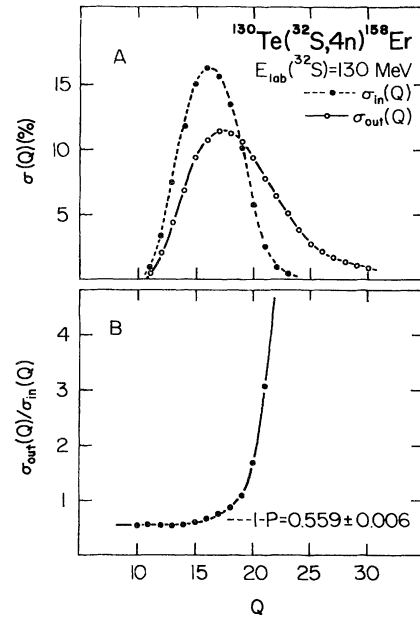


FIG. 3. (a) Sample atomic charge state distributions for ^{158}Er ions produced in the $^{130}\text{Te}(^{32}\text{S},4n)$ reaction at 130 MeV. Measurements made with and without a second carbon foil are identified as $\sigma_{\text{in}}(Q)$ and $\sigma_{\text{out}}(Q)$, respectively. (b) A plot of the ratio $\sigma_{\text{out}}(Q)/\sigma_{\text{in}}(Q)$ vs Q for the data of 3(a). The asymptotic value for low Q is indicated.

ing. This effect has been studied using beams from the accelerator and a theoretical analysis has been made using a semiempirical multiple scattering formalism and the known optical properties of the spectrometer. The theoretical and experimental studies of this effect were in complete agreement and lead to corrections to P which vary from 3% to 8% depending on bombarding energy.

A second source of systematic error relates to possible differences in the equilibration of the atomic charge state distribution in the $10 \mu\text{g}/\text{cm}^2$ carbon backing of the target and the downstream $10 \mu\text{g}/\text{cm}^2$ carbon foil. We have studied this effect using 180 deg elastic scattering reactions well below the Coulomb barrier so that no nuclear effects are present. Reactions of the type $^{168}\text{Er}(^{197}\text{Au},^{168}\text{Er})$ were used to produce particles simulating evaporation residues. Under these conditions the charge state distributions measured with and without the second foil should be identical if a true equilibrium is achieved in each of the carbon foils. We find, however, that $\sigma_{\text{out}}(Q)$ is systematically broader than $\sigma_{\text{in}}(Q)$. Tests with second foils prepared by various techniques and of various thicknesses showed that the observed difference was probably not due to physical differences in the carbon foils. We conclude, therefore, that the broader charge state distribution emerging from the target backing results from its proximity to the violent collision which occurs in the target material and which is absent for the second carbon foil. We have characterized the effect experimentally and have found that an 8% correction to P is required. Within experimental errors this correction is independent of bombarding energy over the range of interest here.

III. RESULTS AND ANALYSIS

A sample of the raw experimental data is shown in Fig. 4 for the $^{154-156}\text{Er}$ isotopes produced in the $^{32}\text{S} + ^{128}\text{Te}$ reaction. Here we plot the observed change in the total internal conversion probability dP per unit change in the bombarding energy dE_{lab} . The horizontal error bars show the energy step used to measure dP while the vertical error bars reflect counting statistics. To a very large degree, systematic errors are eliminated when the difference dP is formed.

The experimental quantities dP/dE can be related to average internal conversion coefficients via the following simple model. First, we assume that the observed value dP is due to the internal conversion probability of the ad-

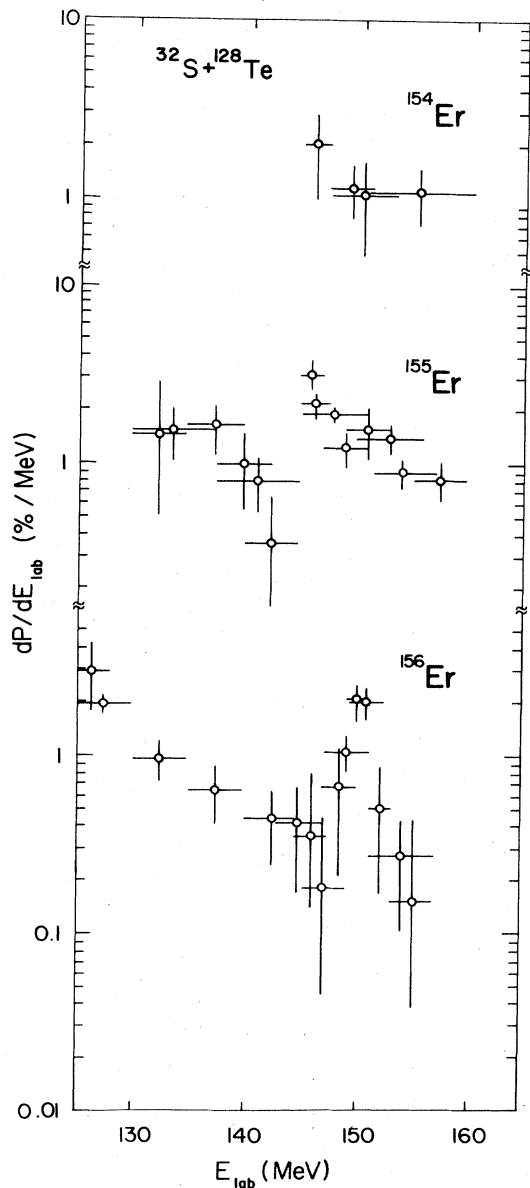


FIG. 4. A sample of dP/dE_{lab} measurements for products of the $^{32}\text{S} + ^{128}\text{Te}$ reaction. The horizontal error bars reflect the energy averaging interval.

ditional γ transitions added at the top of the γ cascade as a consequence of the bombarding energy increase dE_{lab} . This assumption neglects any change in the γ -decay path through the excitation energy-spin plane at low spin which might result from the change in the γ -decay entry region. Studies of yrast region feeding suggest that this assumption is valid for nuclei with reasonably good rotational structure such as those encountered in this work.

The average internal conversion coefficients are most directly related to the quantity dP/dJ where dJ is the increase in the entry region spin associated with the bombarding energy increase dE_{lab} . Thus

$$\frac{dP}{dJ} = \left(\frac{dP}{dE} \right) \left(\frac{dE}{dJ} \right). \quad (6)$$

The first factor on the right-hand side of Eq. (6) comes from experiment while the second factor can be obtained from a statistical model calculation for the reaction. In the present work we used the Monte Carlo statistical model code PACE with parameters adjusted to give an accurate description of the energy dependence of the relative yields and absolute cross sections of the various xn channels. Sample calculated entry region spins for $^{154-156}\text{Er}$ produced in the $^{32}\text{S} + ^{128}\text{Te}$ reaction are shown in Fig. 5. The error bars attached to the calculation indicate the width (standard deviation) of the calculated spin distribution.

γ -ray multiplicity distributions have been measured for this system as a function of bombarding energy. These measurements are in very good agreement with the calculations of Fig. 5. The most extensive test of this code, however, has recently been reported by Sarantites *et al.*,¹² where detailed spin distributions in the Yb isotopes measured with the Oak Ridge spin spectrometer were reproduced with calculations identical to those used here. There are two features of the calculations of Fig. 5 which are important in the present context. First, the inverse

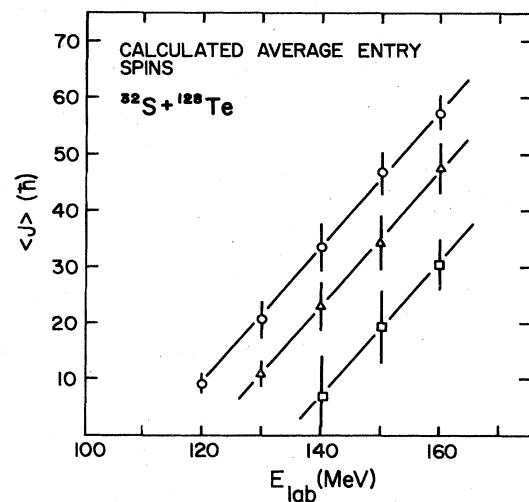


FIG. 5. Sample calculated average entry spins versus bombarding energy for the $^{32}\text{S} + ^{128}\text{Te}$ reaction. $^{156,155,154}\text{Er}$ products are plotted as circle, triangle, and square data points, respectively, while the error bars show the calculated standard deviation of the spin distribution.

slope of the curves gives dE_{lab}/dJ required for Eq. (6). It is noteworthy that this factor is essentially constant for all of the channels considered in the energy range studied here. This fact is virtually independent of the parameters of the calculation. Thus, at worst the transformation from dP/dE_{lab} to dP/dJ may create a small systematic bias in the value of dP/dJ .

The second important feature of the model calculations of $\langle J \rangle$ is their use in relating deduced average internal conversion probabilities to specific regions of spin in the product nuclei. The relationship between $\langle J \rangle$ and E_{lab} is somewhat more sensitive to the model parameters. A wide range of statistical model parameters have been investigated which suggest that $\pm 5\hbar$ is the maximum reasonable uncertainty in $\langle J \rangle$.

In Fig. 6 we plot dP/dJ vs $\langle J \rangle$ for mass 154–158 products. These products are almost exclusively $^{154-158}\text{Er}$ as has been verified by particle- γ coincidence measurements. The sole possible exception to this is the mass 154 products for which significant contamination by ^{154}Ho cannot be ruled out.

The solid lines in Fig. 6 show the expected values of

dP/dJ for stretched $E2$ and $M1$ radiation

$$\frac{dP}{dJ}(E2) = \frac{1}{2} \left[\frac{\alpha_T(E2)}{1 + \alpha_T(E2)} \right] \quad (7)$$

and

$$\frac{dP}{dJ}(M1) = \left[\frac{\alpha_T(M1)}{1 + \alpha_T(M1)} \right], \quad (8)$$

where $\alpha_T(E2)$ and $\alpha_T(M1)$ are the total internal conversion coefficients for $E2$ and $M1$ radiation, respectively. These coefficients have been evaluated at γ -ray transition energies of

$$E_\gamma = \frac{\hbar^2}{2I}(4J - 2)$$

for $E2$ radiation and $\frac{1}{2}$ of this value for $M1$ decay. The moment of inertia I for ^{156}Er and ^{158}Er has been taken from the experimental yrast line up to the highest spin which is known for each nucleus. At higher spins a constant moment of inertia is assumed matched smoothly to

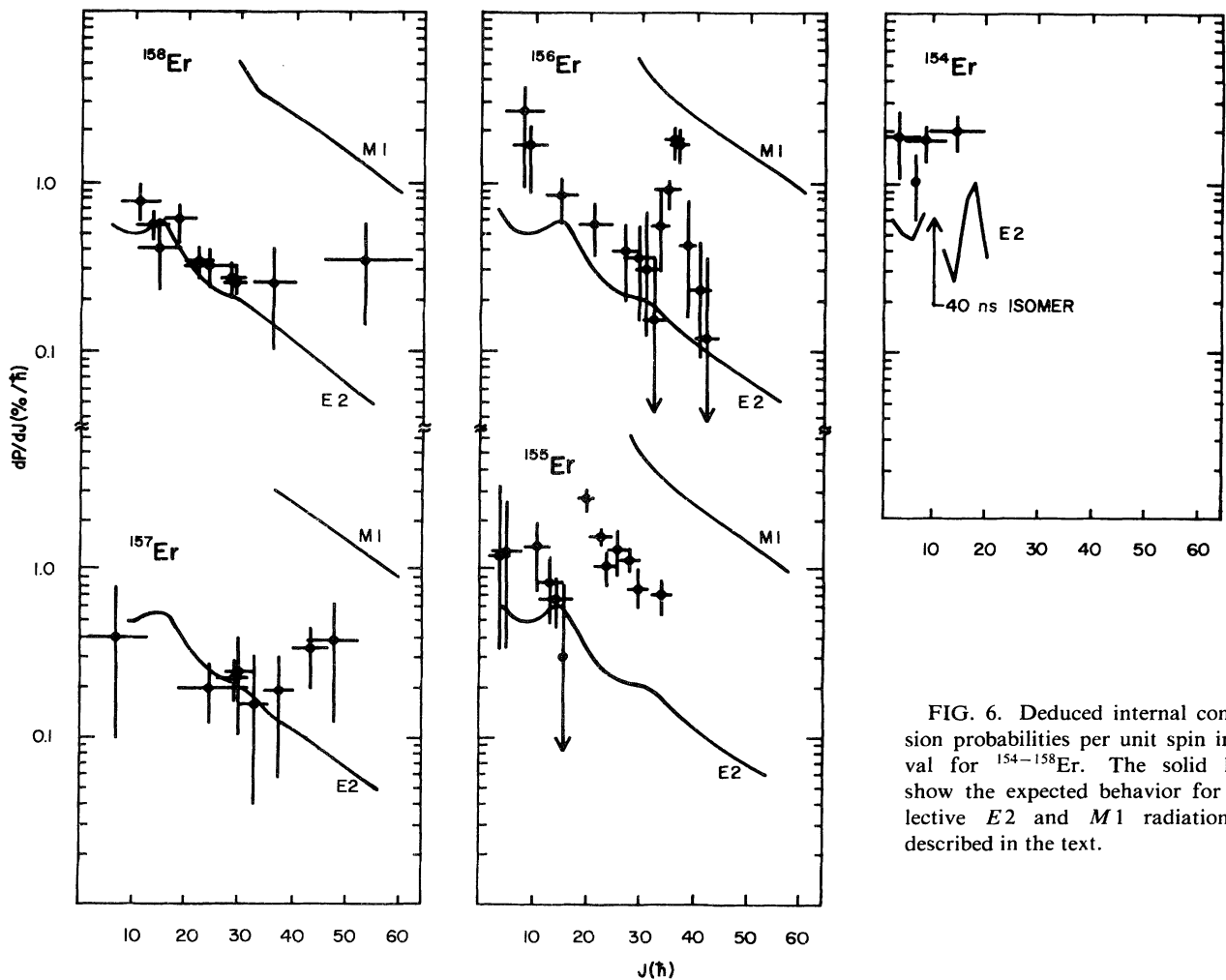


FIG. 6. Deduced internal conversion probabilities per unit spin interval for $^{154-158}\text{Er}$. The solid lines show the expected behavior for collective $E2$ and $M1$ radiation as described in the text.

the experimental yrast line. For ^{155}Er and ^{157}Er , there is insufficient experimental spectroscopic information to permit I to be evaluated in this manner. In these two cases we take I from the neighboring even A isotopes ^{156}Er and ^{158}Er . This is expected on the basis of systematics to be a reasonable procedure except at the very lowest spins for ^{157}Er . The case of ^{155}Er is more complicated in that the yrast line may be expected to be somewhat irregular at low spin as is typical of nuclei nearer the $N=82$ shell closure. At higher spins, however, even ^{155}Er has been shown¹³ to exhibit collective rotational behavior and we estimate that for $J \approx 25\hbar$ the effective moment of inertia for ^{155}Er will not differ significantly from that of ^{156}Er .

The ^{154}Er yrast line is very irregular at low spin but here there is substantial spectroscopic information available. In Fig. 6 we plot dP/dJ for several of the known $E2$ yrast transitions in ^{154}Er . Across this same region of spin, however, there are several mixed $E2/M1$ transitions as well as a 40 ns isomer ($J^\pi=10^-$ or 11^-). Since the γ -ray transition energy out of this isomer is unknown¹⁴ it is impossible to give a proper calculation of dP/dJ across this region. The calculation shown for the known $E2$ transitions is, therefore, a strict lower limit.

IV. DISCUSSION

A. Model dependence of dP/dJ

The virtue of the present results as summarized in Fig. 6 is that they provide an overview of the spin dependence of average continuum internal conversion probabilities for a sequence of light rare earth isotopes. It is important to recognize, however, that the results are strictly model dependent in at least three ways.

(1) It is assumed that dP/dE_{lab} depends only on states at the top of the γ cascade or that the decay flux through the lower spin states is unchanged by a small increase in bombarding energy dE_{lab} .

(2) The magnitude of dP/dJ is proportional to dE_{lab}/dJ which is obtained from a statistical model calculation. Fortunately, this number is largely independent of the details of the model calculation provided the calculations reproduce the energy dependence of the experimental cross sections. We estimate from a study of the parameter dependence of the calculated dE_{lab}/dJ that the model introduces a systematic bias in dP/dJ of $<20\%$.

(3) The correlation of dP/dJ with J again relies on the model calculations. In this case the experimental cross sections supply sufficient constraint to limit the uncertainty in J to $\pm 5\hbar$.

Our analysis of the model dependence of dP/dJ vs J relies primarily on our ability to describe the experimental excitation functions. In fact, however, it is the ability of the calculations to predict reaction product spin distributions which is of importance here. Sarantites *et al.*¹² have studied this question in some detail as mentioned above and find that the code PACE-JULIAN in its form used in the present work gives an excellent reproduction of experimental spin distributions. Their measurements were made in the Yb isotopes, many of which are isotones of the Er products studied here.

B. Excess internal conversion at high spin

As Fig. 6 shows, each of the isotopes $^{155-158}\text{Er}$, for which data exist at high spin, exhibits varying degrees of excess internal conversion at high spin compared to the pure $E2$ limit. The ^{158}Er data span a rather large spin interval. Through the region $15 < J < 40\hbar$ we observe internal conversion probabilities consistent with pure $E2$ radiation along the experimental yrast line. This is not a surprising result. There have been numerous studies of the continuum γ decay¹⁵ of this nucleus in this range of spins all of which indicate collective quadrupole behavior. At higher spins in this nucleus, however, we observe more internal conversion than can be accounted for by continued $E2$ radiation with the same moment of inertia.

The ^{157}Er data exhibit the same behavior with an excess of internal conversion visible for $J > 45\hbar$. At ^{156}Er , however, we observe a striking new behavior. Again we observe internal conversion probabilities at low spin $J < 38\hbar$ which are consistent with virtually pure $E2$ radiation along the experimental yrast line. For $J > 38\hbar$ we observe a dramatic increase in internal conversion which is completely absent again by $J \approx 48\hbar$. Something approaching this singular behavior appears in ^{155}Er beginning at $J \approx 25\hbar$.

The enhanced internal conversion probabilities observed at high spin in the present data, without additional information on the $\langle J \rangle$ dependence of the average γ -ray transition energies, admit at least two interpretations. Either a change in the average γ -ray multipolarity in the direction of enhanced $M1$ radiation occurs or a reduction in the average γ -ray transition energy occurs with continued dominance of $E2$ radiation. Of course, a combination of these two effects cannot be ruled out.

The ^{156}Er data, where the largest excursion of the internal conversion probability is observed, provide the most stringent limitation on these two extreme hypotheses. Interpreted as a change in the $E2$ γ -ray transition energy, the enhanced internal conversion probability observed for ^{156}Er implies a factor of ≈ 3 reduction in the γ -ray energy. Assuming a collective description is still valid, this implies a factor of 3 increase in the moment of inertia. This moment of inertia exceeds by nearly a factor of 3 the liquid drop value at this spin and is therefore unphysical. It is thus highly unlikely that the effect observed in ^{156}Er is due exclusively to low energy collective $E2$ transitions.

We may examine the alternative extreme hypothesis by assuming an unchanged moment of inertia in this high spin region. Interpreted as an effect of collective $M1$ radiation [$E_\gamma(M1) = \frac{1}{2}E_\gamma(E2)$], the ^{156}Er data imply a multipole mixture of $58 \pm 11\%$ $M1$ radiation and $42 \pm 8\%$ $E2$ radiation. The errors quoted here are purely statistical. A similar analysis for the ^{158}Er data yields $20 \pm 13\%$ $M1$ radiation at the highest spins.

Continuum γ -ray measurements for the nuclei studied here will be necessary to further limit interpretations of the observed internal conversion enhancements. Further insight, however, may be had by comparing the present data with the extensive continuum γ -ray spectroscopic studies of the Yb isotopes by Jaaskelainen *et al.*⁷ We will consider in particular ^{160}Yb and ^{158}Yb which are isotones

of ^{158}Er and ^{156}Er , respectively.

The entry region γ decay of ^{160}Yb is observed to proceed mainly through quadrupole radiation for $J < 40\hbar$ as determined by angular anisotropy measurements. At $J = 45\hbar$ a new decay mode appears with a dipole to quadrupole ratio of 0.9 ± 0.2 . This decay mode persists to the highest spin reached in the experiment $\approx 60\hbar$.

The γ decay of ^{158}Yb exhibits predominately quadrupole behavior for $J < 36\hbar$ although the angular distributions are slightly less anisotropic than would be expected for pure stretched quadrupole radiation. At $J = 40\hbar$ a new decay mode appears again characterized by significant dipole competition. This mode is visible in this case, however, only for $40 < J < 48\hbar$. Above this spin the dipole component is absent and the γ spectra again evolve with spin in a manner characteristic of essentially pure stretched quadrupole radiation. Between $J = 40$ and $48\hbar$ the dipole transitions account for 50–60% of the γ rays. In both the ^{158}Yb and ^{160}Yb data the dipole transitions associated with the new decay mode have γ -ray transition energies $\approx \frac{1}{2}$ the corresponding quadrupole transition energy.

The correspondence between the occurrence of dipole transition in the Yb isotopes and enhanced internal conversion observed in the appropriate Er isotone in the present data is quite striking. The narrow spin interval over which dipole transitions at $E_\gamma \approx \frac{1}{2} E_\gamma(E2)$ are observed to account for $\approx 50\%$ of all transitions in ^{158}Yb appears in the isotone ^{156}Er as a similarly narrow interval of enhanced internal conversion. These two observations taken together strongly support a common explanation involving enhanced $M1$ radiation at $\frac{1}{2}$ the $E2$ transition energy. As noted above, in this interpretation, the ^{156}Er data imply a maximum of $58 \pm 11\%$ $M1$ radiation which compares favorably with the observed dipole intensity of 50–60% in ^{158}Yb .

V. CONCLUSIONS

All of the Er isotopes investigated at high spin in this work exhibit enhanced internal conversion which can be consistently interpreted as the onset of a new decay mode involving strong $M1$ competition. The localization of the $M1$ γ -ray transition energies at $\frac{1}{2}$ of the corresponding $E2$ energies implies that significant collectivity remains.

It is tempting to identify the new decay mode with the predicted prolate to oblate shape change discussed in Sec. I. Several qualitative features of the present data and the measurements of Ref. 7 are indeed in accord with such a model including, for example, the gradual reduction of the shape-transition spin for lighter isotopes. There are at least two serious quantitative problems, however.

The γ -ray measurements in the Yb isotopes indicate a strong localization of the $M1$ radiation at $\frac{1}{2}$ the $E2$ energy. This correlation implies continued collective rotation. The $E2$ transition rates have been measured⁶ in the light Er isotopes at high spin and are found to be rather large [$B(E2) > 140$ W.u.]. The cranked shell model calculations, on the other hand, predict deformations of $\epsilon \approx 0.1$ following the prolate to oblate shape transition. In such

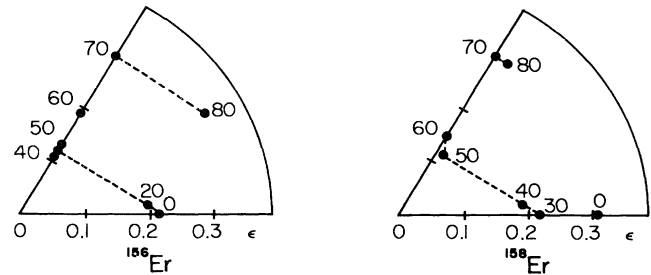


FIG. 7. Calculated equilibrium shapes for ^{156}Er and ^{158}Er in the ϵ - γ plane as a function of spin.

shapes a large fraction of the angular momentum is produced by quasiparticle alignment ($J \approx K$). Under these conditions, the $E2$ transition rate is strongly hindered, hence, the observed $B(E2)$ is hardly consistent with the small predicted deformation. Jaaskelainen *et al.* estimate that oblate deformations as large as $\epsilon \approx 0.3$ would be required to account for the γ -decay data.

A second quantitative problem of the model concerns the rapid disappearance of the new decay mode in both the ^{158}Yb and ^{156}Er data. In ^{156}Er , for example, the oblate shape is predicted by $J = 30\hbar$ at which point $\epsilon \approx 0.1$. Figure 7 shows the predicted equilibrium shapes¹⁷ for ^{158}Er and ^{156}Er in the ϵ - γ plane. The predicted oblate shape is stable in ^{156}Er to $J = 70\hbar$ at which point the nucleus moves quickly through triaxial shapes of large deformation toward fission. Clearly, if the new decay mode is to be associated with the oblate shape then the model seriously overestimates its stability as a function of spin.

It would be premature to speculate whether the problems discussed above point to new physics or whether trivial details of the model are at fault. Indeed it is not clear whether the model is at all appropriate to the description of continuum γ decay at all. These γ transitions are conventionally assumed to occur in an excitation energy window which may extend as much as 10 MeV above the yrast line whereas the model refers to the yrast line itself. The nuclear structure features of the model which are responsible for the stability of the oblate shape clearly wash out at some excitation energy above the yrast line. The extent to which this influences the comparison between theory and experiment is unknown at present. Certainly many interesting theoretical questions remain to be addressed.

At this time there are also many experimental problems to be investigated. More extensive systematics on the occurrence of very high spin $M1$ radiation is required to elucidate the role of the active neutron and proton Nilsson orbitals. Measurements aimed at this question in the Dy and Hf isotopes are in progress. A very important, though difficult, challenge presented by the present data is the observation of the very high spin $M1$ radiation in discrete line spectroscopy and a determination of the associated transition rates.

This work was supported in part by the National Science Foundation and in part by the Alfred P. Sloan Foundation.

- ¹R. M. Diamond and F. S. Stephens, *Annu. Rev. Nucl. Part. Sci.* **30**, 85 (1980), M. J. A. De Voigt *et al.*, *Rev. Mod. Phys.* **55**, 949 (1983).
- ²See, for example, C. G. Andersson *et al.*, *Phys. Scr.* **24**, 266 (1981), and references therein.
- ³L. K. Peker *et al.*, *Phys. Rev. Lett.* **41**, 457 (1978).
- ⁴J. O. Newton and S. H. Sie, *Nucl. Phys.* **A334**, 499 (1980); J. O. Newton *et al.*, *Phys. Rev. Lett.* **40**, 625 (1978); S. H. Sie *et al.*, *Nucl. Phys.* **A352**, 279 (1981).
- ⁵See, for example, S. J. Feenstra *et al.*, *Phys. Lett.* **80B**, 183 (1979); L. Westerberg *et al.*, *Phys. Rev. Lett.* **41**, 96 (1978).
- ⁶D. G. Sarantites *et al.*, *Nucl. Instrum. Methods* **171**, 503 (1980).
- ⁷Markku Jaaskelainen, Ph.D. thesis, University of Jyväskylä, 1983 (unpublished); M. Jaaskelainen *et al.*, *Phys. Lett.* **119B**, 65 (1982), and references therein.
- ⁸T. M. Cormier and P. M. Stwertka, *Nucl. Instrum. Methods* **184**, 423 (1981).
- ⁹T. M. Cormier *et al.*, *Nucl. Instrum. Methods* **212**, 185 (1983).
- ¹⁰F. W. Aston, *Philos. Mag. (London)* **38**, 707 (1939).
- ¹¹See, for example, D. Chmielewska *et al.*, *Nucl. Phys.* **A366**, 142 (1981); Z. Sujkowski *et al.*, *Phys. Lett.* **133B**, 53 (1983).
- ¹²D. G. Sarantites *et al.*, *Phys. Lett.* **115B**, 441 (1982).
- ¹³M. A. Delaplanque *et al.*, *Phys. Rev. Lett.* **43**, 1001 (1979).
- ¹⁴C. Baktash *et al.*, *Phys. Rev. Lett.* **42**, 637 (1979).
- ¹⁵M. A. Deleplanque *et al.*, *Phys. Rev. Lett.* **51**, 1854 (1983), and references therein.
- ¹⁶R. Kroth *et al.*, Institut de Physique Nucléaire (IPN), Orsay, Annual Report, 1982 (unpublished).
- ¹⁷G. Andersson *et al.*, *Nucl. Phys.* **A268**, 205 (1976).